# Dalton Transactions

An international journal of inorganic chemistry

## Accepted Manuscript

Volume 46
Number 10
14 March 2017
Pages 3073-3412

# Dalton Transactions

An international journal of inorganic chemistry

rsc.li/dalton

COMMUNICATION
Douglas W. Stephen et al
N-Heterocyclic carbene stabilized parent sulfenyl, selenenyl, and tellurenyl cations (XH+; X = S, Se, Te)

ISSN 0306-0012

ROYAL SOCIETY OF CHEMISTRY

ROYAL SOCIETY OF CHEMISTRY

rsc.li/dalton

# ARTICLE

# Enhancement of the electrocatalytic abilities toward $CO_2$ reduction by tethering redox-active metal complexes to the active site.

Habib Md. Ahsan,[a,b] Brian K. Breedlove*[a] Cosquer Goulven[c] and Masahiro Yamashita [a,d]

Tethering metal complexes, like[Ru(bpy)$_2$Cl$_2$] (bpy = 2,2`-bipyridine), which are redox-active at low reduction potentials and the ability to transfer electrons to another complex, to a [Ni(cyclen)]$^{2+}$ electrocatalyst enhanced the reduction of $CO_2$ to CO at low overpotentials. The [Ni(cyclen)]$^{2+}$ electrocatalyst was modified by tethering redox-active metal complexes via 4-methyl pyridyl linkers. The redox-active metal complexes were reduced after $CO_2$ bound to the active site. From control potential electrolysis (CPE) experiments in 95:5 (v/v) $CH_3CN/H_2O$, [{([Ru]pic)$_4$cyclen}NiCl]$^{5+}$ ([Ru]$^+$ = {Ru(bpy)$_2$Cl}$^+$; pic = 4-methylpyridyl) could be used to reduce $CO_2$ into CO at turnover frequency (TOF) of 708 s$^{-1}$ with a faradaic efficiency (FE) of 80% at onset potential of −1.60 V vs NHE. At the same time, this electrocatalyst was active at an onset potential of −1.25 V vs NHE, which is the reduction potential of one of the bpy ligands of the [Ru]$^+$ moieties, with FE = 84% and TOF = 178 s$^{-1}$. When the electrocatalysis was performed using [bn$_4$cyclenNiCl]Cl (bn = benzyl) without tethered redox-active metal complexes, TOF was determined to be 8 s$^{-1}$ with FE = 77% at onset potential of −1.45 V vs NHE. The results show that tethering redox-active metal complexes significantly improves the electrocatalytic activities by lowering the potential needed to reduce $CO_2$.

## Introduction

Electrochemical reduction of $CO_2$ to usable compounds, like low molecular mass fuels, etc., still suffers from many challenges, such as low catalytic activities, catalyst stabilities and high overpotentials. Thus, $CO_2$ reduction electrocatalytic systems are needed to overcome the current challenges.[1–5] Metal complexes with macrocyclic ligands have been shown to be electrocatalysts for the reduction of $CO_2$.[6] Eisenberg and co-workers reported nickel and cobalt metal electrocatalysts with 1,4,8,11-tetraazacyclotetradecane (cyclam) ligands in 1980.[7] They reduce $CO_2$ with high current efficiencies to form CO. However, the turnover frequencies (TOFs) in polar solvents, such as water, are low. The mechanisms for these electrocatalysts have been extensively studied. In the case of [Ni(cyclam)]$^{2+}$, the Ni(II) ion becomes a Ni(I) ion, and then $CO_2$ coordinates to it, followed by reduction. Fujita and co-workers have studied the geometric and electronic effects on the catalytic activity using different structural derivatives of [Ni(cyclam)]$^{2+}$.[8] However, [Ni(cyclam)]$^{2+}$ still exhibits a low electrocatalytic activity, and electrocatalysis occurs at high potentials. Many approaches, including the addition of a proton source and modification of the

structure, have been applied to improved electrocatalytic abilities. Saveant and co-workers have reported that a weak Bronsted acid can facilitates the cleavage of a C=O bond in $CO_2$ to produce CO and $H_2O$.[9] Typical proton sources have included $H_2O$, methanol, trifluoroethanol, trifluoroacetic acid and phenol, etc.[10–17] The proton binds to the lone pair of $CO_2$, and the electrons in the double bond move to form a new lone pair to alleviate the positive charge. In other words, after the formation of $CO_2$ adduct, proton-coupled electron transfer or metal ion-coupled electron transfer may occur through the electrocatalyst, followed by protonation. The overall reaction is $CO_2 + 2e^- + 2H^+ \rightarrow CO + H_2O$.

However, modification of the macrocyclic ligands of electrocatalysts may improve their catalytic activities. Saveant and co-workers have reported an iron porphyrin with phenolic groups attached to the porphyrin moiety which electrocatalytically reduces $CO_2$ with high efficiencies at a low overpotential.[9] In addition, [Ni(cyclam–CO$_2$H)]$^{2+}$ (Cyclam-CO$_2$H = 1,4,8,11-tetraazacyclotetradecane-6-carboxylic acid) has been reported to have electrocatalytic activity greater than that of [Ni(cyclam)]$^{2+}$ in acidic media.[12]

In this work, the main focus was to improve electrocatalytic abilities by using a macrocyclic metal complex with redox-active molecules to provide the active site with electrons similar to natural electrocatalysts, like nitrogenase.[18] Herein, [Ru(bpy)$_2$Cl]$^+$ ([Ru]$^+$) was used as the redox-active complex, and a modified [Ni(cyclen)]$^{2+}$ complex was the active site. [bn$_4$cyclenNiCl]Cl (bn = benzyl) was used to demonstrate the effects of the ligand-coordinated redox-active metal complex on the electrocatalytic properties.

## Results and discussion

a. Department of Chemistry, Graduate School of Science, Tohoku University, 6-3 Aza-Aoba, Aramaki, Sendai, 980-8578, Japan.

b. Chemistry Discipline, Science, Engineering and Technology School, Khulna University, Khulna-9208, Bangladesh.

c. Chemistry Department, Graduate School of Science, Hiroshima University, 1-3-1 Kagamiyama, Higashihiroshima, Hiroshima, 739-8526, Japan

d. School of Materials Science and Engineering, Nankai University, Tiajin 300350, China..

e. †Electronic Supplementary Information (ESI) available: $^1H$ NMR, $^{13}C$ NMR, ESI-Mass, X-ray crystallographic data, Diffusion coefficient calculation. CCDC: 1837284 and 1824553 contain supplementary data for this paper.

The electrocatalyst was designed (Fig. 1) while considering enzymes, like nitrogenase, in which the electron source for $N_2$ fixation is bound close to the active site.[18] A 1,4,7,10-tetraazacyclododecane (cyclen) derivative was used as the supporting ligand for the active site toward $CO_2$ reduction due to its rigidity and because it was easy to attach groups, such as 4-methylpyridyl, to the nitrogen atoms using an acid-base reaction.
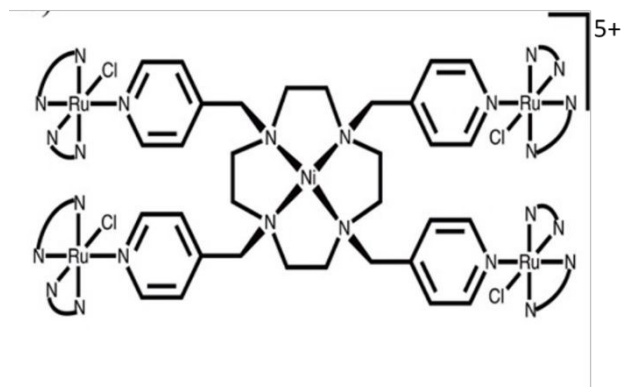


**Fig. 1** Drawing of $[\{([Ru]pic)_4cyclen\}NiCl]^{5+}$ where $[Ru]^+ = [Ru(bpy)_2Cl]^+$ and bpy = 2,2'-bipyridine.

NMR spectroscopy, elemental analysis, and X-ray crystallography were used to characterize the ligand (Experimental section). Then it was attached to $[Ru]^+$ via the 4-methylpyridyl moieties to afford $[([Ru]pic_4cyclen)]^{4+}$, which was coordinated to $NiCl_2$ via a simple ligand substitution reaction. To compare the electrocatalytic abilities with and without tethered redox-active complexes, $bn_4cyclen$ was prepared by using benzyl chloride.[19] $bn_4cyclen$ was fully characterized (Supporting
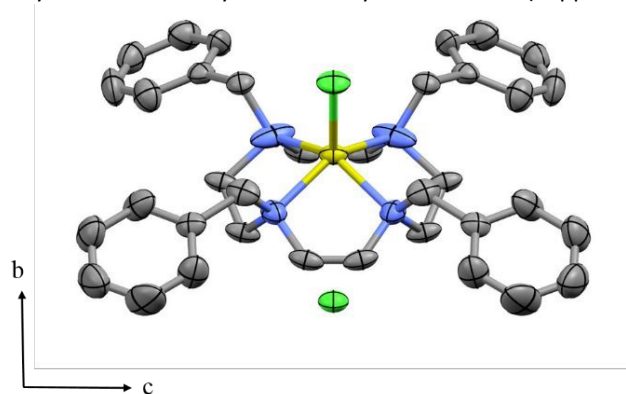


**Fig. 2** ORTEP drawing of $[bn_4cyclenNiCl]Cl$ with the thermal ellipsoids at 50% probability. Disordered carbon atoms and hydrogen atoms were omitted for clarity. Gray: carbon atoms; blue: nitrogen atoms; yellow: nickel atom and green: chloride atoms. Selected bond distance (Å): Planar N–Ni = 0.607; Ni–Cl(1) = 2.254(2); Ni–Cl(2) = 4.597(5); Ni–N(1) = 2.113(8); Ni–N(2) = 2.113(8); Ni–N(3) = 2.107(4) and Ni–N(4) = 2.107(4). Bond angles (deg): N(1)–Ni–Cl(1) = 107.27; N(2)–Ni–Cl(1) = 107.27; N(3)–Ni–Cl(1) = 106.17 and N(4)–Ni–Cl(1) = 106.17.

information). We prepared $[bn_4cyclenNiCl]Cl$ by heating an

ethanolic mixture of $bn_4cyclen$ and $NiCl_2·6H_2O$. Green plate-like crystals were obtained from methanol/diethyl ether.

An ORTEP drawing of $[bn_4cyclenNiCl]Cl$ is shown in Fig. 2 Selected crystal data are summarized in the supporting information. $[bn_4cyclenNiCl]Cl$ crystallized in the orthorhombic space group $Ccm2_1$. The $Ni^{II}$ ion adopted a square-pyramidal like geometry, which was estimated by using the software Smile 2.1 (Table S3 in the SI), and it was determined to be 0.607(6) Å above the plane of four nitrogen atoms of the cyclen ring. Cl(2), which was the counter ion, was located on the opposite side of the apical Cl ion (Ni–Cl (2): 4.59(5) Å).

**Electrochemical properties.** The electrochemical properties of $[([Ru]pic)_4cyclen)]^{4+}$, $[\{([Ru]pic)_4cyclen\}NiCl]^{5+}$, and $[bn_4cyclenNiCl]Cl$ were analyzed under $N_2$ and $CO_2$ by using cyclic voltammetry in anhydrous $CH_3CN$ and 95:5 (v/v) $CH_3CN/H_2O$ containing 0.1 M $TBAPF_6$ as the supporting electrolyte. All potentials are referenced to NHE by referencing the potential of ferrocene vs. NHE.[20] CV of $[([Ru]pic)_4cyclen]^{4+}$ was performed to show the effects of $[Ru]$ on the catalytic process (Fig. 3(A)). Three cathodic waves were observed at −0.65 V, −1.30 V and −1.58 V vs. NHE. The first two waves were assigned to the reduction of bpy to $bpy^−$ by comparing the cyclic voltammograms (CVs) of analogous compounds and $Ru(bpy)_2Cl_2$.[21] The third reduction wave may be due to an electrochemical reaction involving the chloride ligand. The slight increase under $CO_2$ indicates reduction occurred at the ruthenium center. However, this current increase is negligible. Voltammograms of $[\{([Ru]pic)_4cyclen\}NiCl]^{5+}$, shown in Fig. 3(B), were acquired under $N_2$ and $CO_2$ to investigate the electrocatalytic abilities of the complex towards $CO_2$ reduction. Under $N_2$, four reduction waves were observed and assigned by comparing the CVs with those of starting and analogous compounds. The wave at −1.06 V vs. NHE was assigned to the $Ni^{II/I}$ couple,[22] the potential of which was more negative after complexation with $[Ru]^+$. The wave at −1.28 V vs. NHE was assigned to the reduction of a bpy ligand and that at −1.56 V vs. NHE was due to the reduction of the second one. The final wave at −1.78 V vs. NHE was assigned to $Ni^{I/0}$ couple. Under $CO_2$, a large current increase was observed at −1.60 V vs. NHE positive of the $Ni^{I/0}$ wave. This phenomenon was attributed to $CO_2$ binding, where the difference in the potentials under $N_2$ and $CO_2$ atmosphere reflects the ability of the reduced complex to activate $CO_2$.[23,24] In other words, the current is higher than those involving electrocatalysts with other macrocyclic ligands, showing that the $[Ru]^+$ moieties tethered to the electrocatalyst have an electronic effect on the electrocatalysis. The site of electrocatalysis (Ni(II) ion) and the four $[Ru]^+$ moieties are reduced prior to $CO_2$ reduction.

In cyclic voltammograms of $[\{([Ru]pic)_4cyclen\}NiCl]^{5+}$ in 95:5 (v/v) $CH_3CN/H_2O$ (Fig. 3(C)), where $H_2O$ acted as a proton source to facilitate the proton-coupled $CO_2$ reduction,[14] four waves were observed at negative potentials. The wave at −1.02 V vs. NHE was assigned to the reduction of the Ni ion from $Ni^{II}$ to $Ni^{I}$.[22] The reduction wave at −1.25 V vs. NHE was due to the reduction of a bpy ligand of $[Ru]^+$, and that at −1.52 V vs. NHE was assigned to the reduction of the second one. The final wave at −1.75 V vs. NHE was assigned to the reduction of $Ni^{I}$ to $Ni^0$. The wave at

**Journal Name**

**ARTICLE**

−1.75 V shifted positively to −1.60 V, and the current increased dramatically under $CO_2$, indicating that electrocatalytic reduction of $CO_2$ occurred.
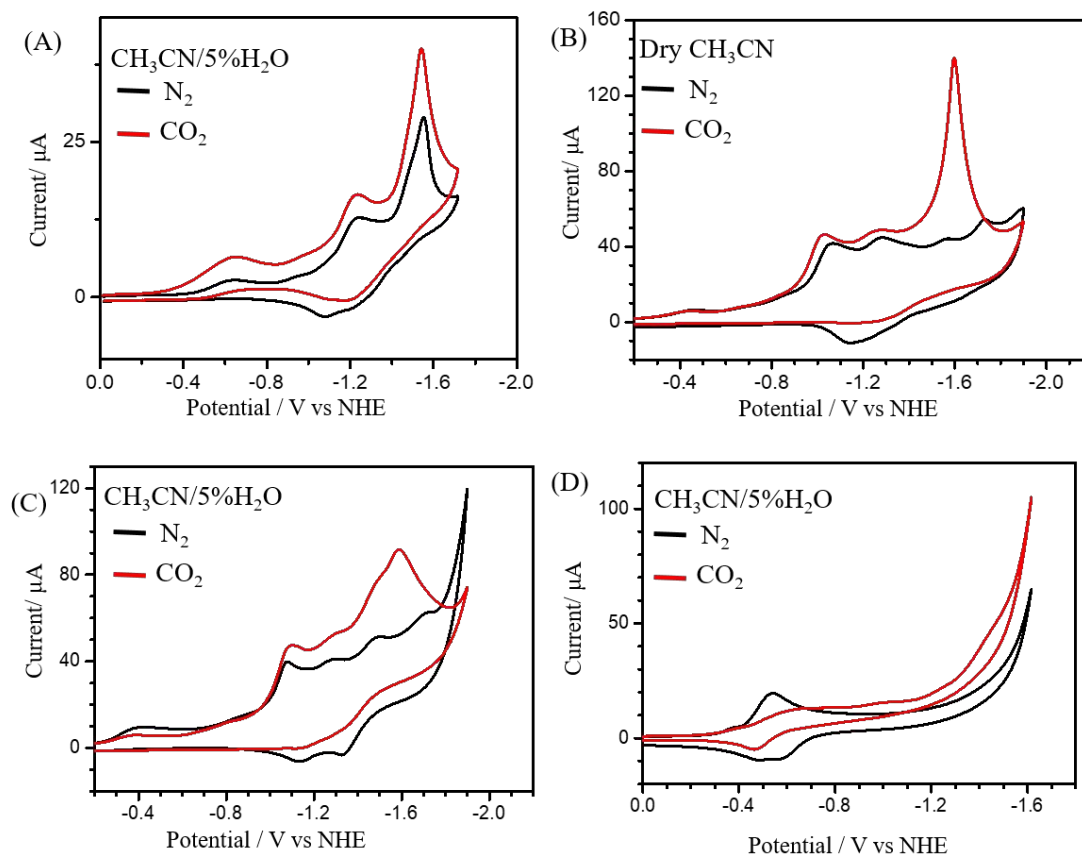


**Fig. 3** Cyclic voltammograms of (A) 1 mM [([Ru]pic)$_4$cyclen]$^{4+}$ in 95:5 (v/v) $CH_3CN/H_2O$, (B) 1 mM [{([Ru]pic)$_4$cyclen}NiCl]$^{5+}$ in $CH_3CN$, (C) 1mM [{([Ru]pic)$_4$cyclen}NiCl]$^{5+}$ in 95:5 (v/v) $CH_3CN/H_2O$, and (D) 1mM [bn$_4$cyclenNiCl]Cl in 95:5 (v/v) $CH_3CN$ containing 0.1 M TBAPF$_6$ at a scan rate of 100 mV/s with a glassy carbon working electrode under $N_2$ (black) and $CO_2$ (red).

In the voltammograms for [bn$_4$cyclenNiCl]Cl in 95:5 (v/v) $CH_3CN/H_2O$ under $N_2$ (Fig. 3(D)), there was a reversible wave at −0.55 V vs. NHE, assigned to the Ni$^{II/I}$ couple. The potential is more positive than that for [Ni(cyclam)]$^{2+}$ and analogs, and this is due to the effects of the benzyl groups attached to the aza N atoms in cyclen.[25] The Ni$^{I/0}$ couple was not observed. The solution was then saturated with $CO_2$, and the cathodic current increased at −1.45 V vs. NHE and shifted positively compared to that under $N_2$. Moreover, it was irreversible, indicating that $CO_2$ reduction occurred. The increase in the catalytic current is similar to that observed using [Ni(cyclam)]$^{2+}$ derivatives in $CH_3CN/H_2O$ solutions.[7,8,25–28] When cyclic voltammetry of a 1:4 mixture of [bn$_4$cyclenNiCl]Cl and Ru(bpy)$_2$Cl$_2$ was examined under similar conditions, only a small increase in the current similar to that of [bn$_4$cyclenNiCl]Cl alone was observed (Fig. S13). The results show that the tethered redox-active complexes greatly affect the electrocatalytic activity.

**Controlled Potential Electrolysis (CPE).** Controlled potential electrolysis (CPE) was carried out using [bn$_4$cyclenNiCl]Cl in a $CO_2$ saturated $CH_3CN$ solution containing 5% $H_2O$ and using [{([Ru]pic)$_4$cyclen}NiCl]$^{5+}$ in $CO_2$ saturated $CH_3CN$ solution with and without 5% $H_2O$, which was used as a proton source. The CPE experiments were performed in a sealed cell using a glassy carbon working electrode. Gaseous products in the headspace of the sealed electrochemical cells were analyzed by using gas chromatography, and the FE value was determined after 30 min of electrolysis. Although FE was determined after 30 min, the catalysts were reasonably stable for at least 6 hours under the conditions used Fig. S11 and S12). CPE was performed at −1.45 V vs. NHE with no electrocatalyst to confirm that electrocatalysis occurred due to the electrocatalyst. Although $CO_2$ binds to the Ni ion at −0.55 V vs. NHE, electrolysis occurs at −1.45 V vs. NHE. Therefore, the CPE experiments in the presence of [bn$_4$cyclenNiCl]Cl were investigated at −1.45 V vs. NHE. After CPE, CO was the only gaseous product, and the FE value was determined to be 77%, which is similar to the FE

values using [Ni(cyclam)]$^{2+}$ analogues.[7,8,25–28] The overpotential using [bn$_4$cyclenNiCl]Cl was calculated to be 730 mV (standard reduction potential for the conversion of $CO_2$ to CO is −0.72 V vs. NHE),[29] and it is similar to previously reported electrocatalysts.

CPE experiments using [{([Ru]pic)$_4$cyclen}NiCl]$^{5+}$ in $CO_2$ saturated $CH_3CN$ solutions were carried out at −1.60 V vs NHE for 30 min, and $CO_2$ was reduced to CO with a FE of 32%. During electrolysis, the solution became cloudy, and a precipitate formed. The precipitate was determined to be $CO_3^{2-}$, which is due the disproportionation of $CO_2$, i.e., $2CO_2 + 2e^- \rightarrow CO + CO_3^{2-}$, by comparing infrared spectra of the precipitate with available carbonate salts.[30] Next, 5% $H_2O$ by volume was added to shut down the disproportionation reaction. CPE was conducted at −1.60 V vs. NHE after saturating the solution with $CO_2$. From headspace analysis, CO was the only gaseous product, and the FE was determined to be 80%. Next, CPE was performed for 30 min at −1.25 V vs. NHE, where a bpy ligand is reduced, and then headspace analysis was used to determine the gaseous products. FE was determined to be 84% for CO. The increase was thought to be because the potential was lower than that to produce $H_2$. The results indicate that tethering redox-active complexes close to the active site decreases the onset potential by about 350 mV.

TOF were calculated from CV and CPE experiments for [bn$_4$cyclenNiCl]Cl and [{([Ru]pic)$_4$cyclen}NiCl]$^{5+}$ using a modified equation reported by McCrory et al. which was first introduced by Saveant and coworkers:[31,32]

$$TOF = \frac{(i_{el})^2 \left(1 + exp\left[\frac{F}{RT}\left(E_{app} - E_{\frac{1}{2}}\right)\right]\right)}{F^2 A^2 D [cat]^2} \quad (1)$$

where $i_{el}$ is the average current of CPE experiment for CO generation ($A$), $F$ is Faraday's constant (96500 $C\,mol^{-1}$), $R$ is the universal gas constant (8.31 $J\,K^{-1}\,mol^{-1}$) , $T$ is the temperature (298 $K$), $E_{app}$ is the applied potential during CPE, $E_{1/2}$ is the standard redox potential of the catalyst, $A$ is the surface area of working electrode (0.94 c$m^2$), $D$ is the diffusion coefficient for catalyst and [$cat$] is the concentration of catalyst in solution (detailed in the supporting information). The TOF values were calculated be 178 s$^{-1}$ and 708 s$^{-1}$ at onset potentials of −1.25 V and −1.60 V vs NHE, respectively, for [{([Ru]pic)$_4$cyclen}NiCl]$^{5+}$, whereas it was 8 s$^{-1}$ at the onset potential of −1.45 V vs NHE for [bn$_4$cyclenNiCl]Cl. TOF for [{([Ru]pic)$_4$cyclen}NiCl]$^{5+}$ is higher by a factor of 88 than that using [bn$_4$cyclenNiCl]Cl, showing the influence of the redox-active metal complexes tethered to the electrocatalyst on the electrocatalytic activity. In addition, [{([Ru]pic)$_4$cyclen}NiCl]$^{5+}$ can be used to the electrocatalytically reduce $CO_2$ at −1.25 V vs NHE, and the TOF value is 22-times higher than that using [bn$_4$cyclenNiCl]Cl. We believe that this is the highest TOF value using azamacrocycle-based electrocatalysts so far reported (Table 4).[16,17,19–23] In addition, the overpotential is lower than those using similar

electrocatalysts. The overpotential decrease of 200 mV for [{([Ru]pic)$_4$cyclen}NiCl]$^{5+}$ is thought to be due to the excess electrons available from the tethered moieties. However, the number of electrons still must be determined. Thus, tethering redox-active metal complexes to catalytic active site is a good way to decrease the overpotential and to improve the electrocatalytic abilities. Although FE is a little lower due to the production of $H_2$, the electrolysis is still reasonably efficient, and the efficiency should increase when a two-compartment cell is used.

## Experimental
### General information
Reagents were purchased from TCI (Tokyo, Japan) and used as is, and solvents were purchased from Wako and used as obtained. [Ru(bpy)$_2$Cl$_2$] was synthesized via a literature procedure.[33] $^1$H and $^{13}$C NMR spectroscopies were performed using a Bruker AV500 and referenced to tetramethylsilane. Tetrabutylammonium hexafluorophosphate (TBAPF$_6$, Aldrich, 98%), recrystallized from hot ethanol, was dried in a vacuum overnight at 90 °C. Mass spectrometry was performed on a Waters Xevo G2 Q-TOF spectrometer equipped with electrospray ionization (ESI). Elemental analyses were performed by the Research and Analytical Center for Giant Molecules of Tohoku University.

*X-ray Crystallography*. Single crystals of compounds were mounted on a glass loop rod with paratone-N (Hampton). A Rigaku Varimax diffractometer equipped with a Saturn724+ CCD detector using graphite monochromated Mo K$\alpha$ radiation ($\lambda$ = 0.71073Å) with a N$_2$ stream was used for data collection. Azimuthal scans of several reflections were used to empirically correct for absorption correction. The data were corrected for Lorentz and polarization effects. Non-hydrogen atoms were refined anisotropically using a least-squares method, and hydrogen atoms at calculated positions were refined using a riding model. SHELXTL was used for structure refinement.

*Electrochemistry*. An ALS/HCH Model 620D electrochemical analyzer was used for the electrochemical experiments. A glassy carbon (3 mm diameter) electrode was used as a working electrode, Pt wire was used as a counter electrode, and Ag wire was used as a pseudo reference electrode. Tetrabutylammonium hexafluorophosphate (TBAPF$_6$) (0.1 M) in 95:5 (v/v) $CH_3CN/H_2O$ was used as the electrolyte. N$_2$ and $CO_2$ were bubbled into the solutions for at least 30 min before cyclic voltammetry was performed. Ferrocene was used as an internal standard for referencing the potentials to NHE.[20]

*Controlled Potential Electrolysis*. Controlled potential electrolysis (CPE) experiments were performed using an ALS/HCH Model 620D electrochemical analyzer. A Gamry five-neck cell equipped with three Ace-Thread ports for each electrode and two joints for gas purging and gas collection after electrolysis was used for the CPE experiments. A glassy carbon electrode with a surface area of 0.94 cm$^2$ was used for the working electrode. Pt wire was used for the auxiliary electrode, and Ag wire was used as a pseudo-reference electrode, both of which were separated from the bulk solution by a porous frit.

TBAPF$_6$ (0.1 M) in 95:5 (v/v) CH$_3$CN/H$_2$O was used as the electrolyte. CO$_2$ was bubbled into the solution for 30 min before electrolysis. Gas samples were acquired using a gas-tight syringe and injected into a gas chromatograph (Agilent 6890N, 5975C) equipped with Agilent HP-MOLESIEVE columns (length 30 m, ID, 0.32 mm, film 12 μm) to determine the products of CPE. The carrier gas was helium (99.99%). The detector was a mass spectrometer with an *m/z* range of 10–100. Calibration curves for determining the amount of CO produced were prepared. The faradaic efficiency (FE) was calculated by using eq 1.[19] The TOF and FE values are reported as averages of three CPE runs.

$$n[CO] = \frac{Q_{el} \times FE}{nF} \qquad (2)$$

where n[CO] is the moles of CO generated from electrolysis (A), $Q_{el}$ is the charge passed during electrolysis (C) and $F$ is Faraday's constant (96,500 C mol$^{-1}$) and $n$ is number of electrons used to convert CO$_2$ to CO, which is a 2-electron process.

### Synthesis of 1,4,7,10-Tetra(4-methylpyridyl)-1,4,7,10-tetraazacyclododecane (pic$_4$cyclen)

To a solution of 1,4,7,10-tetraazacyclododecane tetrahydrochloride (318 mg, 1 mmol) in 20 mL deionized water was added to an aqueous solution of 0.2 N NaOH to adjust the pH to 12. 4-Methylpyridyl chloride hydrochloride (820 mg, 5 mmol) was slowly added while maintaining the pH at 12. The solution was stirred for 24 h during which time a pink solid formed. The pink solid was collected by filtration and washed with water (10 mL) and ether (10 mL). Pure pic$_4$cyclen was obtained from dichloromethane/hexane. Yield: 76%. ESI-MS: *m/z* 537.34 (C$_{32}$H$_{40}$N$_8$). Elemental anal. calcd for C$_{32}$H$_{40}$N$_8$: C, 71.61; H, 7.51; N, 20.88%. Found: C, 71.52; H, 7.42; N, 20.53%. $^1$H NMR (CDCl$_3$, $\delta$): 8.45 (d, 2H), 7.32 (d, 2H), 3.44 (s, 2H), 2.69 (t, 4H). $^{13}$C NMR (CDCl$_3$, $\delta$): 53.45, 59.00, 149.10, 123.60, 149.68.

### Synthesis of [([Ru]pic$_4$cyclen)]$^{4+}$

Ru(bpy)$_2$Cl$_2$ (452 mg, 0.94 mmol) was dissolved in a mixture of water (5 mL) and ethanol (20 mL) in a 50 mL pear-shaped flask, and the solution was degassed with N$_2$ for 10 min. After heating the solution for 30 min at 75 °C, pic$_4$cyclen (100 mg, 0.19 mmol) dissolved in ethanol (5 mL) was added slowly. The solution was then refluxed at 100 °C for 72 h after which the solvent was removed on a rotary evaporator. Next, the resulting residue was dissolved in a minimal amount of water, and the desired complex precipitated when excess NH$_4$PF$_6$ was added. The remaining ammonium salt was removed, and the product was purified by using size-exclusion column chromatography with bio-Beads S-X1. Yield: 63%. ESI-MS (*m/z*): 583.09. Elemental anal. calcd for [C$_{112}$H$_{104}$Cl$_4$F$_{24}$N$_{24}$P$_4$Ru$_4$]·CH$_3$CH$_2$OH·2H$_2$O: C, 44.73; H, 3.84; N, 11.23%. Found: C, 45.69, H, 3.87; N, 11.21%.

### Synthesis of [{[Ru]pic$_4$cyclen}NiCl]Cl[PF$_6$]$_4$

A solution of [([Ru]pic$_4$cyclen)]$^{4+}$ (291 mg, 0.1 mmol) and NiCl$_2$·6H$_2$O (28 mg, 0.12 mmol) in ethanol (15 mL) in a 50 mL pear-shaped flask was heated at 75 °C for 6 h. A black-red precipitate formed. The solid was collected by filtration, washed with ether (5 mL) and then dried in vacuo overnight. Yield: 82%. Elemental anal. calcd for [C$_{112}$H$_{104}$Cl$_6$F$_{24}$N$_{24}$P$_4$NiRu$_4$]·2H$_2$O·3CH$_3$CH$_2$OH: C, 44.07; H, 3.95; N, 10.45%. Found: C, 44.03, H, 3.99; N, 10.48%.

### Synthesis of bn$_4$cyclen

To a solution of 1,4,7,10-Tetraazacyclododecane tetrahydrochloride (447 mg, 1.5 mmol) and potassium carbonate (2.07 g, 15 mmol) in boiling anhydrous acetonitrile (50 mL), a solution of benzylchloride (0.76 mL, 6.6 mmol) in acetonitrile (10 mL) was added dropwise.[32] Then the reaction mixture was reflux for 12 h. After cooling to room temperature, the solid that formed during the reaction was removed by filtration. The filtrate was evaporated to dryness. The product was extracted with boiling heptane (2 × 50 mL). The extracts were combined, and the solvent was removed under reduced pressure. The product was recrystallized from acetonitrile. Yield: 77%. Elemental anal. calcd. for C$_{36}$H$_{44}$N$_4$: C, 81.16; H, 8.32; N, 10.52%. Found: C, 80.99; H, 8.34; N, 10.57%. $^1$H NMR (CDCl$_3$, $\delta$): 2.68 (s, 16 H), 3.42 (s, 8H), 7.18–7.36 (m, 20H). $^{13}$C NMR (CDCl$_3$, $\delta$): 53.01, 60.10, 126.51, 1128.00, 128.91, 149.68 140.09.

### Synthesis of [bn$_4$cyclenNiCl]Cl

bn$_4$cyclen (53 mg, 0.1 mmol) and NiCl$_2$·6H$_2$O (28.45 mg, 0.12 mmol) were added to a 50 mL pear-shaped flask containing ethanol (20 mL). The solution was heated at 60 °C for 6 h. A greenish yellow color precipitate formed. The solid was collected by filtration and washed with a small amount of ethanol. The compound was recrystallized from methanol and diethyl ether by slow evaporation. Yield 82%. Elemental anal. calcd. for C$_{36}$H$_{44}$N$_4$NiCl$_2$: C, 65.28; H, 6.70; N, 8.46%. Found: C, 64.92; H, 6.72; N, 8.50%.

## Conclusions

We showed that tethering redox-active complexes to an electrocatalysis enhanced the electrocatalytic abilities towards CO$_2$ reduction. CO$_2$ reduction was investigated with [{([Ru]pic)$_4$cyclen}NiCl]$^{5+}$ and [bn$_4$cyclenNiCl]Cl. Both electrocatalysts can be used to reduce CO$_2$ to CO in the presence of H$_2$O as a proton source. The FE and TOF values are higher than those using [bn$_4$cyclenNiCl]Cl. The redox-active metal complexes are reduced after CO$_2$ binds to the electrocatalytic active site. In other words, there should be more electrons available to the active site, which would enhance the electrocatalytic activity. [bn$_4$cyclenNiCl]Cl had electrocatalytic abilities similar to those of [Ni(cyclam)]$^{2+}$, whereas those of the electrocatalyst with tethered redox-active complexes were significantly better.

## Author Contributions

The manuscript was written through contributions of all authors. All authors have given approval to the final version of the manuscript. Experiments were performed by B. K. B. and H. M. A., Crystal data were analyzed H. M. A, B. K. B and C. G and the manuscript was prepare by all four authors.

## Conflicts of interest

There are no conflicts to declare.

## Acknowledgements

## Notes and references

1   K. L. Materna, R. H. Crabtree and G. W. Brudvig, *Chem. Soc. Rev.* 2017, **46**, 6099–6110.
2   J. Qiao, Y. Liu, F. Hong and J. Zhang, *Chem. Soc. Rev.,* 2014, **43**, 631–675.
3   M. Aresta and A. Dibenedetto, *Dalton Trans.* 2007, 2975–2992.
4   J. Albo, M. Alvarez-Guerra, P. Castaño and A. Irabien, *Green Chem.* 2015, **17**, 2304–2324.
5   H. Takeda, C. Cometto, O. Ishitani and M. Robert, *ACS Catal*. 2017, **7,** 1, 70–88.
6   S. Meshitsuka, M. Ichikawa and K. Tamaru, *J. Chem. Soc., Chem. Commun*. 1974, 158–159.
7   B. J. Fisher and R. Eisenberg, *J. Am. Chem. Soc*. 1980, **102**, 7361–7363.
8   J. Schneider, H. Jia, K. Kobiro, D. E. Cabelli, J. T. Muckerman and E. Fujita, *Energy Environ. Sci*. 2012, **5**, 9502–9510.
9   C. Costentin, S. Drouet, M. Robert and J. M. Savéant, *Science,* 2012, **338**, 90–94.
10  K. T. Ngo, M. McKinnon, B. Mahanti, R. Narayanan, D. C. Grills, M. Z. Ertem and J. Rochford, *J. Am. Chem. Soc*. 2017, **139**, 2604–2618.
11  M. L. Clark, K.E. Grice, C. E. Moore, A.L. Rheingold and C. P. Kubiak, *Chem. Sci.* 2014, **5**, 1894–1900.
12  G. Neri, I. M. Aldous, J. J. Walsh, L. J. Hardwick and A. J. Cowan, *Chem. Sci*. 2016, **7**, 1521–1526.
13  M. D. Sampson and C. P. Kubiak, *J. Am. Chem. Soc*. 2016, **138**, 1386–1393.
14  J. M. Smieja, M. D. Sampson, K. A. Grice, E. E. Benson, J. D. Froehlich and C. P. Kubiak, *Inorg. Chem*. 2013, **52**, 2484–2491.
15  C. W. Machan, M. D. Sampson and C. P. Kubiak, *J. Am. Chem. Soc*. 2015, **137**, 8564–8571.
16  S. L. Hooe, J. M. Dressel, D. A. Dickie, and C. W. Machan, *ACS Catal*. 2020, 10, 1146–1151.
17  X. Su, K. M. McCardle, L. Chen, J. A. Panetier and J. W. Jurss, *ACS catal*. 2019, 9, 7398–7408.
18  B. K. Burgess and D. J. Lowe, *Chem. Rev*. 1996, **96**, 2983–3012.
19  V. O. Gelmboldt, E. V. Ganin, S. S. Basok, E. Y. Kulygina, M. M. Botoshansky, V. C. Kravtsov and M. S. Fanari, *CrystEngComm*. 2011, **13**, 3682–3685.
20  V. V. Pavlishchuk. And A. W. Addison, *Inorganica Chimica Acta.* 2000, **298**, 97–102.
21  V. Leigh, W. Ghattas, R. Lalrempuia, H. Müller-Bunz, M. T. Pryce and M. Albrecht, *Inorg. Chem*. 2013, **52**, 5395–5402.
22  E. Kimura, X. Bu, M. Shionoya, S. Wada and S. Maruyama, *Inorg. Chem.* 1992, **31**, 4542–3546.
23  D. A. Gangi and R. R. Jr Durand, *J. Chem. Soc., Chem. Commun*. 1986, 697–699.
24  M. H. Schmidt, G. M. Miskelly and N. S. Lewis, *J. Am. Chem. Soc.* 1990, **112**, 3420–3426.
25  J. D. Froehlich and C. P. Kubiak, *Inorg. Chem*. 2012, **51**, 3932–3934.
26  B. J. Fisher and R. Eisenberg, *J. Am. Chem. Soc*. 1980, **102**, 7361–7363.
27  M. Beley, J. P. Collin, R. Ruppert and J. P. Sauvage, *J. Am. Chem. Soc*. 1986, **108**, 7461–7467.
28  J. D. Froehlich and C. P. Kubiak, *J. Am. Chem. Soc*. 2015, **137**, 3565–3573.
29  C. Cometto, L. Chen, P. K. Lo, Z. Guo, K. C. Lau, E. A. Mallart, C. Fave, T. C. Lau and M. Robert, *ACS Catal*. 2018, **8**, 3411–3417.
30  R. J. Haines, R. E. Wittrig and C. P. Kubaik, *Inorg. Chem*. 1994, **33**, 4723–4728.
31  W. Nie, and C. C. L. McCrory, *Chem. Commun*. 2018, **54**, 1579–1582.
32  C. Costentin, M. Robert and J. M. Savéant, *Chem. Soc. Rev.* 2013, **42**, 2423–2436.
33  G. A. Lawrance, D. R. Stranks, and S. Suvachittanont, *Inorg. Chem*. 1978, **17**, 3322–3325.